In Vivo Manifestation of Notch Related Phenotypes in Zebrafish Treated with Alzheimer's Amyloid Reducing γ-Secretase Inhibitors

Ting Yang[1], **Dilyara Arslanova**[1], **Xiaoyin Xu**[2], **Yue-Ming Li**[3], and **Weiming Xia**[1]

[1]Center for Neurologic Diseases, Department of Neurology, Harvard Medical School, Boston, MA

[2]Department of Radiology, Brigham and Women's Hospital, Harvard Medical School, Boston, MA

[3]Molecular Pharmacology & Chemistry Program, Memorial Sloan-Kettering Cancer Center, New York, NY

Abstract

γ-Secretase is responsible for the final cleavage of amyloid precursor protein to generate the amyloid-β protein, the major component of plaques in the brains of Alzheimer's disease patients. γ-Secretase inhibitors (GSI) have been explored for therapeutic inhibition of Aβ generation, but mechanistic toxicity has been documented due to its blockage of γ-secretase cleavage of several dozens of substrates including Notch. This becomes the primary obstacle for most inhibitors during the preclinical development and the main concern for several compounds in the clinical trials. To predict potential side effects related to Notch signaling, we examined global effect of GSIs in vertebrate animal zebrafish. We have used two potent GSIs (GSI A and GSI 18) with a sub-μM effective concentration for 50% Aβ inhibition (EC50). Zebrafish embryos were treated with GSI A, 18 or a well characterized GSI DAPT, and transparent animals were examined for up to 7 days. GSI A had less abnormal phenotype in zebrafish, compared to GSI 18-treated embryos that displayed curved tails, a loss of pigmentation, and reduced swim bladder and heart rate. To understand mechanistic effect at the molecular level, we examined Notch signaling in these GSI-treated zebrafish. Notch phenotypes were observed in embryos treated with 50 and 10 μM GSI 18, but not with 10 μM GSI A. In accordance, in situ hybridization with a probe against Notch target gene her6 showed a weaker staining in embryos treated with 10 μM GSI 18 than those treated with 10 μM GSI A. In conclusion, phenotypic profile in whole animals offers important information on Notch related pathways and provides prediction of safe compounds during early development stages of therapeutic GSIs.

INTRODUCTION

Alzheimer's disease (AD) is pathologically characterized by the presence of extracellular neuritic plaques and intracellular neurofibrillary tangles (Selkoe 1999). While the neurofibrillary tangles are mainly composed of hyperphosphorylated Tau protein, the neuritic plaques are formed by a gradual accumulation of amyloid β protein (Aβ). Among

Address correspondence to: Weiming Xia, Ph.D., Center for Neurologic Disease, Harvard Institutes of Medicine, HIM 616, 77 Avenue Louis Pasteur, Boston, MA 02115, Tel. 617 525-5200, Fax. 617 525-5252, wxia@rics.bwh.harvard.edu.

various Aβ isoforms, the most common ones are 40-residue Aβ (Aβ40) and 42-residue Aβ (Aβ42). Aβ is produced by sequential cleavage of amyloid precursor protein (APP) by β-secretase and γ-secretase (Selkoe 1999, Xia 2001), and the γ-secretase is responsible for the final cleavage to generate Aβ at residue 40 or 42. The γ-secretase is composed of presenilins (PS1 or its analogue PS2), presenilin enhancer (Pen-2), nicastrin, and Aph-1 (Wolfe *et al.* 1999, Francis *et al.* 2002, Yu *et al.* 2000). So far, all autosomal dominant mutations have only been found in PS and APP genes, and missense mutations in PS and APP genes account for the majority of early onset familial AD cases. Therefore, γ-secretase is considered a key protease involved in the pathogenesis of AD and is one of the most promising therapeutic targets for AD treatment.

The identification of γ-secretase as the target for blocking Aβ production was established by earlier discoveries that loss of PS1 (De Strooper *et al.* 1998) or its critical aspartate residues (Wolfe *et al.* 1999) leads to a blockage of Aβ generation. Besides APP, γ-secretase cleaves many substrates such as Notch (De Strooper *et al.* 1999). The protease complex cleaves Notch to generate Notch intracellular domain, which is critical for proper neuronal development. The differentiation of these two substrates by the γ-secretase complex is under intensive investigation, and selective compound that blocks Aβ production without affecting Notch signaling would be ideal.

Regulation of γ-secretase cleavage of APP and Notch could be modulated by co-factors like TMP21 (Chen *et al.* 2006) or by pharmacologic manipulation. In a cell free system, cultured cells including rat primary neuronal cultures and in guinea pig brain, the Abl kinase inhibitor Gleevec (imatinib mesylate) has been shown to reduce Aβ production (Netzer *et al.* 2003). This is not related to the Abl kinase activity, as no difference in Aβ reduction was detected in fibroblasts cultured from wildtype versus Abl knockout mice, indicating a unique mechanism independent of its kinase inhibitory effect. Importantly, Gleevec does not inhibit the γ-secretase mediated S3 cleavage of Notch-1 (Netzer *et al.* 2003). Therefore, Gleevec functions as a selective γ-secretase inhibitor that specifically blocks Aβ production without affecting the γ-secretase cleavage of Notch.

It is believed that selective GSI like Gleevec does not bind to the active site of the protease, but evidence is absent for its binding to the substrate. On the contrary, previous studies have shown that another group of APP selective GSIs, NSAIDs, could specifically bind to APP, which makes it distinguishable from other substrates like Notch (Kukar *et al.* 2008). By a mechanism of selectively binding to APP, NSAIDs specifically block Aβ production without affecting the Notch cleavage and downstream signaling (Weggen *et al.* 2001, Kukar *et al.* 2008).

Altered phenotypes from abnormal Notch signaling are among the most studied molecular events in animal models. In zebrafish, a number of Notch mutants display defective anteroposterior polarity and increased neurogenin 1 (ngn1) positive cells. Defective somitogenesis and neurogenesis lead to curved tails and reduction in neural crest cell migration, which further cause a loss of pigmentation (Jiang *et al.* 1996, van Eeden *et al.* 1996). These phenotypes can be replicated in zebrafish treated with a potent GSI, DAPT, at the late blastula stage (Geling *et al.* 2002). Besides DAPT, the Aβ-lowering JLK non-

peptidic isocoumarin inhibitors (Petit *et al.* 2003) and compound E (Yang *et al.* 2008) were also tested for their effect on the Notch pathway responsible for somitogenesis in the zebrafish embryo.

The use of zebrafish for toxicity assessment has been widely accepted and put in practice (Zon & Peterson 2005). Mechanistic toxicity associated with GSI has been the main concern for compounds that are undergoing preclinical development and clinical trials, as the GSIs block γ-secretase that cleaves several dozens of substrates (Xia & Wolfe 2003). Treating mice with a potent γ-secretase inhibitor for 15 days results in many unwanted side effects, such as impaired lymphocyte development, and increased goblet cell number in intestine with abnormal tissue morphology (Wong *et al.* 2004). In zebrafish, intestinal development is most likely tied to swim bladder development, as both intestine and swim bladder arise from the same progenitor cells (Holtzinger & Evans 2005). It has been shown that a downstream effecter of Notch, Hey-2, regulates Gata4 activity, and both Gata4 and Gata6 regulate the formation of multiple organs in zebrafish, including the swim bladder (Holtzinger & Evans 2005). Zebrafish cardiovascular system is also regulated in part by Notch signaling. For example, a zebrafish mutant termed *gridlock* exhibits disrupted aortic blood flow that mimicked features of aortic coarctation in humans, and the mutant gene is at the downstream of Notch signaling (Zhong *et al.* 2001).

In this study, we characterized two potent GSIs, GSI A and GSI 18, in zebrafish. GSI A is identical to compound X, which was used to explore adipsin as a non-invasive Notch responding marker protein from plasma and feces of compound-treated animals (Searfoss *et al.* 2003). Treatment of rats with compound X at doses much higher than those required for Aβ42 reduction leads to a gastrointestinal toxicity characterized by an increase in goblet cell number (Searfoss *et al.* 2003). GSI 18 has been used to block Notch signaling in earlier studies (Fan *et al.* 2006, Lewis *et al.* 2005). Because most side effects associated with a new compound are almost unpredictable before being dosed to animals, an alternative approach would be to treat transparent vertebrate zebrafish and predict possible side effects. In this study, we used GSI A, GSI 18 and DAPT to treat zebrafish and analyzed various phenotypes, some of which are not directly related to Notch signaling. We found that GSI A, with an EC50 at 1.6 nM in cultured cells, caused less phenotypic alteration in zebrafish, comparing to GSI 18 that showed stronger phenotypes.

METHODS

Embryo Treatment

Embryos were placed in a 24-well plate (5–6 embryos/well). Compounds were dissolved in 1 mL of egg water (final concentration at 50 μM, 10μM and 1μM for DAPT {N-[N-(3,5-Difluorophenacetyl-L-alanyl)]-S-phenylglycine t-Butyl Ester}, GSI A (Searfoss *et al.* 2003) and GSI 18 (Fan et al. 2006, Lewis et al. 2005), 0.1% DMSO was used as a negative control). Embryo medium was replaced with the compound containing egg water, and the embryos were incubated at 28°C overnight before survival rate was recorded and photographic images were taken. Compounds were applied at 24 hours post-fertilization (hpf). Prior to the treatment at 24 hpf, embryos were de-chorionated in pronase.

Blocking Aβ production by γ-secretase inhibitors

Compounds were dissolved in the DMEM growth media and applied to ~90% confluent APP-expressing CHO cells in 96-well plates. After incubation for 4–5 hours at 37°C, cells were centrifuged for 5 minutes at 6000 g, and supernatant media were collected for Aβ measurement by ELISA. Sandwich ELISAs for monomeric Aβ were performed as described (Johnson-Wood *et al.* 1997). The capture antibodies 2G3 (to Aβ residues 33–40) and 21F12 (to Aβ residues 33–42) were used for Aβ40 and Aβ42 species. The detecting antibody was biotinylated 266 (to Aβ residues 13–28). These antibodies were kindly provided by Dr. P. Seubert and Dr. D. Schenk (Elan, plc).

In Vitro γ-Secretase Activity Assay

The *E. coli* generated APP-based, 100-residue γ-secretase substrate C100 -Flag was purified as previously described (Esler *et al.* 2002, Fraering *et al.* 2004, Campbell *et al.* 2005). C100-Flag substrate contains an initiating methionine, 99 amino acids that start at the BACE cleavage site, and a Flag tag. The membrane vesicles were solubilized in 1% CHAPSO-HEPES and diluted in a final concentration of 0.2% CHAPSO-HEPES. Phosphatidylethanolamine (PE) and phosphatidylcholine (PC) were added to the final concentration of 0.02% PE and 0.08% PC. After adding DMSO or test compounds to the solubilized γ-secretase complex, substrate C100-Flag was added to the mixture, then followed by incubation at 37°C for 4 hour. AICD was detected by Western blot using antibody against the Flag tag, as previously described (Esler et al. 2002).

The Notch signaling activity was measured in human embryonic kidney (HEK) 293 cells expressing *Hes-1* reporter construct (Hes-Luc) that was generated by inserting three of Su(H) binding sequence in the pGL3-pro luciferase reporter vector (Promega, Madison, WI). Transfected cells were treated with γ-secretase inhibitors GSI A, GSI 18 or DAPT for 8 hr, followed by the measurement of luciferase activity (Luciferase Assay System, Promega, Madison, WI), as previously reported (Yang *et al* 2008).

Conventional Microscope Imaging

Compound-treated embryos were observed under an OLYMPUS SZX12 microscope. For examination, embryos were removed from the compound-containing medium and placed in 0.4% tricane (3-amino benzoic acid ethyl ester, Sigma, St. Louis, MO) solution. Upon anesthetizing, embryos were placed in 3% methylcellulose for positioning and images were recorded with an OLYMPUS Q-COLOR3 camera.

In situ Hybridization

In situ hybridization of compound-treated embryos was carried out at 2 dpf using the probe against *her6* gene. Single-stranded RNA probes against *her6* were synthesized from a cDNA clone (provided by Dr. P Raymond, University of Michigan, Ann Arbor, MI) using T7 RNA polymerase after linearization by restriction digest. The probe was then labeled with digoxigenin-UTP (Roche, Basel, Switzerland). At least 10 to 20 embryos were examined for each experiment. Images were taken at 64x magnification for stained embryos.

Heart rate, pigmentation and swim bladder Analysis

Zebrafish embryos were treated with secretase inhibitors at various concentrations. The embryos were placed on their side for videotaping. Heart rate, in beats per minute, was determined by extrapolating the heart rate per 15 sec on the video. The intensity of pigmentation was quantified in a semi-automatic approach by first drawing region of interest (ROI) on an image followed by segmentation from other areas. After segmenting the pigmentation, the total area and average pixel values of pigmentation were calculated. The values of the DMSO treated embryos were used as the benchmark for comparison. The size of swim bladder was quantified by drawing a region of interest over the swim bladder followed by the calculation of the area. All calculations were performed using MATLAB (MathWorks, Natick,MA).

RESULTS

Inhibition of γ-secretase activity in cultured cells treated with GSIs

Two GSIs (Fig. 1A) and a widely used control GSI, DAPT, were applied in our studies. An APP overexpressing CHO cell line 7W was treated with individual compounds and the levels of secreted Aβ in the media were measured by ELISA. Levels of Aβ40 and Aβ42 in the media of 7W cells that were treated with 0.1% DMSO were normalized to 1 and used to calculate the relative levels of Aβ from cells treated with DAPT, GSI A, or GSI 18. As expected, cells treated with DAPT showed an inhibition of the generation of Aβ40 and Aβ42 (Fig. 1B, C). Interestingly, GSI A showed a much stronger inhibition on Aβ40 and Aβ42 production than DAPT, while GSI 18 was less potent than DAPT in inhibiting Aβ40 and Aβ42 production. While all three GSIs had sub-μM effective concentration of 50% inhibition of Aβ generation (EC50, GSI 18=0.78 μM, DAPT=0.1 μM), GSI A showed strongest inhibition with EC50 at 1.6 nM.

When the *E. coli* generated APP-based, 100-residue γ-secretase substrate C100-Flag was mixed with the membrane vesicles solubilized in CHAPSO, AICD could be detected by Western blotting with a Flag antibody in the presence of DMSO (Fig. 2A). DAPT at 10 μM also inhibited AICD generation, while substrate alone was not converted to AICD in the absence of γ-secretase (Fig. 2A, "Sub alone"). A dose-dependent inhibition of AICD generation by GSI A was detected (Fig. 2A), and generation of AICD was inhibited in the presence of 10μM of GSI 18 (Fig. 2B).

We further examined an inhibitory effect of GSIs on the γ-secretase cleavage of Notch. Notch signaling and levels of NICD can be quantified using a *Hes-1* reporter construct (Hes-Luc) that was generated by insertion of three Su(H) binding sequences in the pGL3-pro luciferase reporter vector, as we have previously reported (Yang *et al*, 2008). A construct encoding a truncated, γ-secretase immediate substrate Notch E was transiently co-transfected with Hes-Luc reporter construct into HEK293 cells, and transfected cells were treated with different concentrations of GSIs. We found that luciferase activities were inhibited by high doses of GSI A, GSI 18 and DAPT (Fig. 2C). While the inhibition of Notch signaling in these cells was less efficient compared to Aβ blockage, essentially we did not see a dramatic difference in potency among three GSIs in cultured cells (Fig. 2C).

Phenotype alteration in embryos treated with increasing concentrations of potent GSIs

To predict *in vivo* Notch related side effect, we tested these GSIs in a whole animal, zebrafish. A large cluster of zebrafish embryos were routinely generated, and several dozen embryos were treated with each compound. First, we used a conventional microscope to monitor embryo survival from 1 dpf to 7 dpf and assess the effects of these compounds on the zebrafish death rate. Two treatment paradigms were applied, i.e., embryos treated at 6 hours post fertilization (hpf) or 24 hpf. We found that treatment of embryos during earlier developmental stages (6 hpf) caused severe damage to embryos, and a high number of embryos could not survive through 2 or 3 dpf (data not shown). When embryos were treated at 24 hpf, much less embryos were succumbed to the compound and died. Therefore, we examined all embryos treated with GSIs at 24 hpf.

The zebrafish embryos were treated with different concentrations of DAPT, GSI A or GSI 18. The phenotypes of zebrafish embryos treated with increasing concentrations of three compounds were compared at 2 dpf (Fig. 3) and 3 dpf (Fig. 4). The major phenotypes we examined were curved tail and pigmentation. Images of the treated embryos were acquired using a stereomicroscope, and both dorsal and lateral views of zebrafish embryos were acquired.

Embryos treated with DAPT showed curved tails, bent trunks, smaller eyes (Fig. 3A), compared to control embryos (treated with 0.1% DMSO) that showed a wild-type phenotype (Fig. 3B). The curvature was obvious when a lateral view of zebrafish was obtained. Embryos treated with 50 μM GSI A (Fig. 3C) or GSI 18 (Fig. 3D) showed defective phenotypes. GSI 18 caused stronger phenotypes in zebrafish than GSI A and DAPT did. Embryos treated with 10 μM of GSI 18 showed curved trunks, less pigmentations, smaller eyes, curved and short tails (Fig. 3D). These phenotypes were not observed in embryos treated with 10 μM GSI A or DAPT (Fig. 3A and C).

Abnormal phenotypes of embryos treated with 50 μM DAPT persisted into 3 dpf (Fig. 4A), while DMSO did not have any effect on zebrafish (Fig. 4B). Embryos treated with 50 μM or 10 μM GSI 18 continued to show the curvature of the tails, and even more obvious than that at 2 dpf (Fig. 4D). For GSI A-treated embryos, most fish displayed curved and short tails, smaller eyes at 50 μM, but none at 10 μM (Fig. 4C).

The dramatic difference between GSI A and GSI 18 treated embryos could be further illustrated by acquisition of images of all embryos treated with each compound at 10 μM (Fig. 4E). Apparently, all embryos treated with 10 μM GSI 18 showed curved tails, while none of GSI A treated embryos showed curved tails. Therefore, 10 μM GSI A did not affect animals to a level that would cause significant impairment in normal embryonic development.

Heart rate analysis of zebrafish embryos

When we examined transparent GSI-treated embryos, we noticed a weaker heart beat in some of GSI-treated embryos. We video-recorded the heart beats of groups of GSI-treated embryos and searched for abnormal phenotypes associated with heart development. Heart rate, in beats per minute, was determined by extrapolating the number of heart beats per 15

sec on the video. We found that the reduction of heart rates in the presence of GSIs were dose dependent (Fig. 5A and B). In particular, DAPT had most severe effect at later development stages (Fig. 5C). All DAPT-treated embryos did not show clear heart beat at 4 dpf (Fig. 5C), although the blood flow was not disrupted. The DAPT-treated embryos showed abnormal heart movement that pushed blood flow through heart chamber, which kept animal alive (data not shown). At 2 and 3 dpf, 50μM DAPT-treated embryos showed significantly slower heart beat than those treated with GSI A or GSI 18. GSI 18 had more severe effect than GSI A, and the heart rate in 50 μM GSI 18-treated embryos was significantly lower than that of 50 μM GSI A-treated embryos (Fig. 5C). Comparing to DMSO treated embryos, all GSI-treated embryos had a significant drop of heart rate at 2, 3 and 4 dpf.

Size of swim bladder was reduced in embryos treated with GSIs

The air-filled swim bladder first formed as a single chamber, which inflated at 1–3 dpf, when the body length reached 3.5–4 mm. Embryos treated with 50 μM GSIs did not reveal any swim bladder and could not be quantified (data not shown). When 10 μM GSIs were utilized and compound treated embryos were kept until 7dpf, we found that each compound had different effect on the loss of swim bladder during different development stages. When the size of swim bladder was quantified using MATLAB, we normalized the size of swim bladder from embryos treated with DMSO to 1. At 3 dpf, GSI A did not alter the size of swim bladder (92±6%, mean±SEM), while GSI 18 reduced the size of swim bladder to 73±11% compared to those of DMSO treated embryos. However, the difference between GSI and DMSO treated embryos was not statistically significant. At 4 dpf, swim bladders of embryos treated with GSI A or GSI 18 remained similar sizes. Only at 5 dpf did embryos treated with GSI A show a significant reduction in size of swim bladder (37±14%). Similarly, the size of embryos treated with GSI 18 reduced to 18±4%, only ~1/5th of those of DMSO treated embryos. The swim bladders of embryos treated with GSIs remained at the same small size through day 6 and 7. The difference between GSI A and GSI 18 treated embryos was not significant. DAPT treated embryos showed a significant reduction of size and had swim bladder at half size of those treated with DMSO (56±9%) at 3 dpf. The swim bladders of these embryos remained at the same small size from day 3 to day 7. Therefore, embryos treated with GSI 18 had relatively smaller size of swim bladder, comparing to those of embryos treated with GSI A.

Relative levels of pigmentation in embryos treated with GSIs

Black pigment cells, or melanocytes, are the major contributing cells to pigmentation in vertebrate organisms. To explore the effect of compound on pigmentation of zebrafish, we used a conventional microscope and quantified segment with MATLAB from 4dpf to 6dpf. Embryos were treated with these three compounds at 50 μM, 10 μM and 5 μM. Embryos treated with GSI 18 at 50 μM were transparent, and we defined the level of pigmentation as 0. The level of pigmentation of embryos treated with DMSO was normalized to be 100%.

Embryos treated with 10 μM DAPT showed a relative ~70% pigment density compared to the levels of pigment in embryos treated with DMSO (Fig. 6A). At 50 μM, DAPT treated embryos only showed ~30% relative levels of pigment compared to control DMSO treated

embryos. Similar reduction of pigmentation was observed at the later stages (Fig. 6B and C). At 6 dpf, embryos treated with 50 μM GSIs showed similar levels of reduction in pigmentation that resulted in almost transparent animals. Apparently, treating embryos with GSIs at a high concentration for a longer period, e.g., 5 days, had a dramatic effect on pigment formation, and its reduction reached the maximum level to make the animal transparent. To search for statistically significant difference in the efficacy of these GSIs, we examined the approximate concentrations of GSIs that could reduce 50% of pigmentation. We found that the effective concentration for 50% reduction of pigmentation was 5–10 μM for GSI 18, which was lower than those for GSI A and DAPT. On average, DAPT and GSI A had similar effect on pigment formation, and the effective concentration to achieve 50% pigment reduction was above 10 μM but below 50 μM. Overall, GSI 18 showed relatively more potent inhibition on pigmentation during embryonic development.

Co-relate Notch signaling to global phenotypic alteration

The overall phenotypes associated with GSI-treated zebrafish reflected an abnormal Notch signaling, e.g., zebrafish rely on Notch signaling activity throughout embryonic and metamorphic development for the formation of pigmentation. To corroborate the Notch phenotypes associated with curved trunk/tail and decreased pigmentation, we analyzed mechanistic effect on Notch signaling by GSI A and GSI 18, i.e., the expression levels of the Notch downstream target gene *her6* was measured by *in situ* hybridization using a *her6* probe.

In DMSO-treated embryos, *her6* expression was mainly clustered in the ventral midbrain and ventral hindbrain. When embryos were treated with GSI A at 10 μM, a weaker staining of *her6* was observed. When embryos were treated with a lower concentration of GSI A at 1 μM, those embryos showed a very similar *her6* staining pattern to the control embryos. However, in the presence of 10 μM GSI 18, the *her6* expression was much reduced in most areas, reflecting a strong inhibition of γ-secretase activity. At the lower concentration of GSI 18 (1 μM), almost no difference was observed between GSI 18 and DMSO treated embryos (Fig. 7A). We segmented the regions of interest, i.e., regions with high *her6* expression such as dorsal diencephalon, retinas, ventral midbrain and hindbrain, telencephalon, olfactory vesicles, branchial arches, and pectoral fins. When the expression levels of *her6* in DMSO treated zebrafish were normalized to 1, a significant reduction in relative levels of *her6* expression in zebrafish treated with 10 μM GSI A or GSI 18 was observed. The inhibitory effect of GSI 18 was significantly stronger than that of GSI A (Fig. 7B). When the *her6* staining is linked to morphological alterations (Fig. 3 and Fig. 4), the level of reduction in Notch signaling is closely linked with the severity of phenotypes that was observed in these zebrafish. For example, a loss of *her6* staining in the presence of 10 μM GSI 18 corresponded to stronger phenotypes at 2 and 3 dpf, comparing to those treated with 10 μM GSI A (Fig. 3C, D and 4C, D, E).

DISCUSSION

Identifying AD targets for therapeutic intervention has been an ongoing endeavor for the past century, and enzymes responsible for Aβ generation are among the most promising

ones. The amyloid hypothesis has evolved to the stage that is widely supported by genetic, biochemical and immunohistochemical evidences (Hardy & Selkoe 2002). While activation of α-secretase will theoretically increases non-amyloidogenic processing of APP, amyloidogenic β- and γ-secretases are two prime targets for blocking Aβ generation.

The crystal structure of β-secretase has been elucidated (Hong *et al.* 2000), but identifying a potent β-secretase inhibitor that can efficiently cross blood brain barrier is still a challenge. The crystal structure of the γ-secretase, on the other hand, is difficult to obtain, and previous studies have started to shed light on its structural arrangement of all four components (Lazarov *et al.* 2006). While a reasonable number of potent GSI have been synthesized, an excellent GSI selective for APP processing yet awaits for identification and further optimization. Non-selective blockage of Notch signaling by existing GSIs has been the major obstacle and accounts for the most mechanistic toxicities observed in GSI-dosed animals.

To predict toxicity of GSIs in a vertebrate animal, we treated zebrafish with two GSIs that showed potent EC50 when used to treat cultured cells (Fig. 1). The standard procedures for testing compounds in zebrafish have been applied in this study, and we found that these GSIs did not cause extensive embryonic lethality when embryos were treated at 24 hpf. GSIs treated embryos survived through day 7, which provided us a wide window to observe the anatomy of developing zebrafish (Fig. 3 and Fig. 4). Apparently, microscopic images of zebrafish have revealed much detailed information about potential abnormalities caused by an inhibition of γ-secretase. While a loss of swim bladder may not be the cause of embryonic lethality, it reflects a system-wide alteration in the presence of GSI. Mechanistic analysis of the phenotypic profile suggests that most abnormalities were related to the inhibition of γ-secretase cleavage of Notch by GSIs.

In zebrafish, the same progenitor cells develop into swim bladder and intestine, which are downstream of Notch signaling (Holtzinger & Evans 2005). The reduction of heart rate, which might be the leading cause of death in a small number of embryos, is also linked to Notch signaling. The *gridlock* gene is at downstream of Notch signaling (Zhong *et al.* 2001), and the dysfunctional gridlock in the absence of Notch signaling might be in part responsible for these phenotypes (Fig. 5). Apparently, the development of zebrafish cardiovascular system is extremely complicated, and the *gridlock* mutant zebrafish showed disrupted aortic blood flow that only partially resembled the phenotype we have observed in GSI-treated embryos (Zhong *et al.* 2001). Thus, it is unlikely that dysfunctional gridlock would be the sole cause for these phenotypes.

Direct effect from abnormal Notch signaling is evident in GSI-treated embryos. We have previously reported phenotypes of zebrafish that were knocked down of individual γ-secretase components (Campbell *et al.* 2006) or expressed truncated Pen-2 (Zetterberg *et al.* 2006). These phenotypes caused by dysfunctional γ-secretase and subsequent Notch signaling are consistent with earlier reports on Notch mutant zebrafish (Jiang *et al.* 1996, van Eeden *et al.* 1996). Those embryos treated with high concentrations of GSI failed normal somitogenesis and neurogenesis, two key events that lead to curved tails and reduction in neural crest cell migration, which caused a loss of pigmentation (Fig. 6). Using

these two readouts, we characterized the properties of GSI A and GSI 18 and examined their effect on Notch signaling in a whole animal.

In situ hybridization of GSI-treated zebrafish with a probe against Notch target gene *her6* (Fig. 7) provided a molecular basis to the abnormal phenotypes associated with defective Notch signaling during zebrafish development. Both GSI A and GSI 18 were able to block γ-secretase in whole animals and reduce *her6* staining. Comparing to embryos treated with GSI A at 10 μM, GSI 18 was more potent in inhibiting Notch signaling in embryos, which showed a stronger reduction in *her6* staining. This was consistent with GSI 18-induced stronger phenotypic changes in developing zebrafish embryos. Interestingly, cultured cell-based Luciferase activity assay did not reveal significant difference in their inhibition of Notch signaling. These results emphasize the need of animal test to determine the mechanistic toxicities associated with Notch signaling. The difference might come from different absorption and metabolization of the compounds. In contrast to mice and guinea pigs, it is difficult to harvest brains from zebrafish embryos to measure the drug levels, making it impractical to compare the exposure of our compounds in zebrafish and mammals.

Our results indicate that GSI A was more potent in inhibiting Aβ generation but induced less phenotypic changes in developing zebrafish embryos than GSI 18. Further studies are needed to identify the target of GSI A by performing binding assays to understand the site of action within γ-secretase complex. Previous report has shown that nicastrin is not only required for γ-secretase cleavage of APP and Notch (Francis et al. 2002, Lee *et al.* 2002, Siman & Velji 2003, Shirotani *et al.* 2003, Li *et al.* 2003) but also serve as an initial binding partner for γ-secretase substrates like APP and Notch (Shah *et al.* 2005). Another γ-secretase component, Pen-2, has been found to modulate the formation of PS1 versus PS2 containing γ-secretase complex (Placanica *et al.* 2008), and an artificial elongation of the Pen-2 N terminus increased Aβ42 production (Isoo *et al.* 2007). In addition, C-terminus of Pen-2 is critical for intermolecular interactions and function of presenilin complexes (Hasegawa *et al.* 2004, Kim & Sisodia 2005). Therefore, Pen-2 might play a role to influence the selective cleavage of APP by γ-secretase. Recent studies have shown a critical role of Aph-1B in regulating the γ-secretase cleavage of APP (Serneels *et al.* 2005). Knockout of each of the three Aph-1 homologous genes (Aph-1A, B, and C) in mice leads to divergent phenotypes, suggesting that different γ-secretase complexes *in vivo* may exert separate biological functions (Serneels *et al.* 2005). In mammalian cultured cells and zebrafish, it is not clear whether GSI A specifically blocked one isoform of γ-secretase that is responsible for APP processing. The structure of GSI A is different from coumarin and does not like coumarin dimer-based compounds that bind to the allosteric site of the γ-secretase (Shelton *et al.* 2009). However, its structure is similar to that of compound E, which was shown to bind to PS1 (Seiffert *et al.* 2000). It is conceivable that GSI A may similarly bind to PS1 fragments. Alternatively, GSI A may have a substrate preference like some NSAIDs which prefer APP over other substrates (Kukar et al. 2008), and a direct interaction of GSI and the APP inhibitory domain (Tian *et al.* 2010) could also lead to a modulation of γ-secretase cleavage and Aβ production.

It is important to understand how zebrafish absorb and metabolize GSIs that showed significant impact on embryonic development. As two or more species are used for

bioefficacy determination, our test in zebrafish provides important information on GSIs that warrants further studies in a second animal model, such as transgenic mouse or guinea pig. Zebrafish essentially provide a unique tool to predict potential outcomes for future animal studies, where positive outcomes will lead us one step closer to a successful amyloid-based therapy.

ACKNOWLEDGMENT

ABBREVIATIONS

AD	Alzheimer's disease
Aβ	amyloid β protein
APP	amyloid precursor protein
Abl	Abelson leukemia
dpf	days post fertilization
EC	effective concentration
GSI	γ-secretase inhibitor
hpf	hours post fertilization
NICD	Notch intracellular domain
PS	Presenilin
TMD	transmembrane domain
WB	Western blot

REFERENCE

Campbell, W.; Wolfe, M.; Xia, W. Assays for Amyloid Precursor Protein γ-Secretase Activity. In: Xia, W.; Xu, H., editors. Amyloid Precursor Protein, A Practical Approach. Boca Raton: CRC Press; 2005. p. 51-68.

Campbell WA, Yang HW, Zetterberg H, Baulac S, Sears JA, Liu T, Wong STC, Zhong TP, Xia W. Zebrafish lacking Alzheimer Presenilin Enhancer 2 (Pen-2) demonstrate excessive p53 dependent apoptosis and neuronal loss. J Neurochem. 2006; 96:1423–1440. [PubMed: 16464238]

Chen F, Hasegawa H, Schmitt-Ulms G, et al. TMP21 is a presenilin complex component that modulates gamma-secretase but not epsilon-secretase activity. Nature. 2006; 440:1208–1212. [PubMed: 16641999]

De Strooper B, Annaert W, Cupers P, et al. A presenilin-1-dependent gamma-secretase-like protease mediates release of Notch intracellular domain. Nature. 1999; 398:518–522. [PubMed: 10206645]

De Strooper B, Saftig P, Craessaerts K, Vanderstichele H, Gundula G, Annaert W, Von Figura K, Van Leuven F. Deficiency of presenilin-1 inhibits the normal cleavage of amyloid precursor protein. Nature. 1998; 391:387–390. [PubMed: 9450754]

Esler WP, Kimberly W, Ostaszewski B, Ye W, Diehl T, Selkoe D, Wolfe MS. Activity dependent isolation of the presenilin-g-secretase complex reveals nicastrin and a g substrate. Proc Natl Acad Sci. 2002; 99:2720–2725. [PubMed: 11867728]

Fan X, Matsui W, Khaki L, Stearns D, Chun J, Li YM, Eberhart CG. Notch pathway inhibition depletes stem-like cells and blocks engraftment in embryonal brain tumors. Cancer Res. 2006; 66:7445–7452. [PubMed: 16885340]

Fraering PC, LaVoie MJ, Ye W, Ostaszewski BL, Kimberly WT, Selkoe DJ, Wolfe MS. Detergent-dependent dissociation of active gamma-secretase reveals an interaction between Pen-2 and PS1-NTF and offers a model for subunit organization within the complex. Biochemistry. 2004; 43:323–333. [PubMed: 14717586]

Francis R, McGrath G, Zhang J, et al. aph-1 and pen-2 are required for Notch pathway signaling, g-secretase cleavage of bAPP and presenilin protein accumulation. Dev Cell. 2002; 3:85–97. [PubMed: 12110170]

Geling A, Steiner H, Willem M, Bally-Cuif L, Haass C. A gamma-secretase inhibitor blocks Notch signaling in vivo and causes a severe neurogenic phenotype in zebrafish. EMBO Rep. 2002; 3:688–694. [PubMed: 12101103]

Hardy J, Selkoe DJ. The amyloid hypothesis of Alzheimer's disease: progress and problems on the road to therapeutics. Science. 2002; 297:353–356. [PubMed: 12130773]

Hasegawa H, Sanjo N, Chen F, et al. Both the sequence and length of the C terminus of PEN-2 are critical for intermolecular interactions and function of presenilin complexes. J Biol Chem. 2004; 279:46455–46463. [PubMed: 15322109]

Holtzinger A, Evans T. Gata4 regulates the formation of multiple organs. Development. 2005; 132:4005–4014. [PubMed: 16079152]

Hong L, Koelsch G, Lin X, Wu S, Terzyan S, Ghosh AK, Zhang XC, Tang J. Structure of the protease domain of memapsin 2 (beta-secretase) complexed with inhibitor. Science. 2000; 290:150–153. [PubMed: 11021803]

Isoo N, Sato C, Miyashita H, Shinohara M, Takasugi N, Morohashi Y, Tsuji S, Tomita T, Iwatsubo T. Abeta42 overproduction associated with structural changes in the catalytic pore of gamma-secretase: common effects of Pen-2 N-terminal elongation and fenofibrate. J Biol Chem. 2007; 282:12388–12396. [PubMed: 17329245]

Jiang YJ, Brand M, Heisenberg CP, et al. Mutations affecting neurogenesis and brain morphology in the zebrafish, Danio rerio. Development. 1996; 123:205–216. [PubMed: 9007241]

Johnson-Wood K, Lee M, Motter R, et al. Amyloid precursor protein processing and A beta42 deposition in a transgenic mouse model of Alzheimer disease. Proc Natl Acad Sci U S A. 1997; 94:1550–1555. [PubMed: 9037091]

Kim SH, Sisodia SS. A sequence within the first transmembrane domain of PEN-2 is critical for PEN-2-mediated endoproteolysis of presenilin 1. J Biol Chem. 2005; 280:1992–2001. [PubMed: 15537629]

Kukar TL, Ladd TB, Bann MA, et al. Substrate-targeting gamma-secretase modulators. Nature. 2008; 453:925–929. [PubMed: 18548070]

Lazarov VK, Fraering PC, Ye W, Wolfe MS, Selkoe DJ, Li H. Electron microscopic structure of purified, active gamma-secretase reveals an aqueous intramembrane chamber and two pores. Proc Natl Acad Sci U S A. 2006; 103:6889–6894. [PubMed: 16636269]

Lee S, Shah S, Li H, Yu C, Han W, Yu G. Mammalian APH-1 Interacts with Presenilin and Nicastrin, and is Required for Intramembrane Proteolysis of APP and Notch. J. Biol.Chem. 2002; 277:45013–45019. [PubMed: 12297508]

Lewis SJ, Smith AL, Neduvelil JG, et al. A novel series of potent gamma-secretase inhibitors based on a benzobicyclo[4.2.1]nonane core. Bioorg Med Chem Lett. 2005; 15:373–378. [PubMed: 15603957]

Li T, Ma G, Cai H, Price DL, Wong PC. Nicastrin Is Required for Assembly of Presenilin/gamma -Secretase Complexes to Mediate Notch Signaling and for Processing and Trafficking of beta -Amyloid Precursor Protein in Mammals. J Neurosci. 2003; 23:3272–3277. [PubMed: 12716934]

Netzer WJ, Dou F, Cai D, et al. Gleevec inhibits beta-amyloid production but not Notch cleavage. Proc Natl Acad Sci U S A. 2003; 100:12444–12449. Epub 12003 Oct 12441. [PubMed: 14523244]

Petit A, Pasini A, Alves Da Costa C, et al. JLK isocoumarin inhibitors: selective gamma-secretase inhibitors that do not interfere with notch pathway in vitro or in vivo. J Neurosci Res. 2003; 74:370–377. [PubMed: 14598313]

Placanica L, Tarassishin L, Yang G, Peethumnongsin E, Kim SH, Zheng H, Sisodia S, Li YM. PEN2 and Presenilin-1 Modulate the Dynamic Equilibrium of Presenilin-1 and Presenilin-2 gamma - Secretase Complexes. J Biol Chem. 2008; 25:25.

Searfoss GH, Jordan WH, Calligaro DO, et al. Adipsin, a biomarker of gastrointestinal toxicity mediated by a functional gamma-secretase inhibitor. J Biol Chem. 2003; 278:46107–46116. [PubMed: 12949072]

Seiffert D, Bradley JD, Rominger CM, et al. Presenilin-1 and -2 are molecular targets for gamma-secretase inhibitors. J Biol Chem. 2000; 275:34086–34091. [PubMed: 10915801]

Selkoe DJ. Translating cell biology into therapeutic advances in Alzheimer's disease. Nature. 1999; 399(Supp):A23–A31. [PubMed: 10392577]

Serneels L, Dejaegere T, Craessaerts K, et al. Differential contribution of the three Aph1 genes to {gamma}-secretase activity in vivo. Proc Natl Acad Sci U S A. 2005; 102:1719–1724. [PubMed: 15665098]

Shah S, Lee SF, Tabuchi K, et al. Nicastrin functions as a gamma-secretase-substrate receptor. Cell. 2005; 122:435–447. [PubMed: 16096062]

Shelton CC, Zhu L, Chau D, Yang L, Wang R, Djaballah H, Zheng H, Li YM. Modulation of gamma-secretase specificity using small molecule allosteric inhibitors. Proc Natl Acad Sci U S A. 2009; 106:20228–20233. [PubMed: 19906985]

Shirotani K, Edbauer D, Capell ASJ, Steiner H, Haass C. gamma -Secretase Activity Is Associated with a Conformational Change of Nicastrin. J Biol Chem. 2003; 278:16474–16477. [PubMed: 12644462]

Siman R, Velji J. Localization of presenilin-nicastrin complexes and gamma-secretase activity to the trans-Golgi network. J Neurochem. 2003; 84:1143–1153. [PubMed: 12603837]

Tian Y, Bassit B, Chau D, Li YM. An APP inhibitory domain containing the Flemish mutation residue modulates gamma-secretase activity for Abeta production. Nat Struct Mol Biol. 2010; 17:151–158. [PubMed: 20062056]

van Eeden FJ, Granato M, Schach U, et al. Mutations affecting somite formation and patterning in the zebrafish, Danio rerio. Development. 1996; 123:153–164. [PubMed: 9007237]

Weggen S, Eriksen JL, Das P, et al. A subset of NSAIDs lower amyloidogenic Abeta42 independently of cyclooxygenase activity. Nature. 2001; 414:212–216. [PubMed: 11700559]

Wolfe MS, Xia W, Ostaszewski BL, Diehl TS, Kimberly WT, Selkoe DJ. Two transmembrane aspartates in presenilin-1 required for presenilin endoproteolysis and γ-secretase activity. Nature. 1999; 398:513–517. [PubMed: 10206644]

Wong GT, Manfra D, Poulet FM, et al. Chronic treatment with the gamma-secretase inhibitor LY-411,575 inhibits beta-amyloid peptide production and alters lymphopoiesis and intestinal cell differentiation. J Biol Chem. 2004; 279:12876–12882. Epub 12004 Jan 12876. [PubMed: 14709552]

Xia W. Amyloid metabolism and secretases in Alzheimer's disease. Curr Neurol Neurosci Rep. 2001; 1:422–427. [PubMed: 11898552]

Xia W, Wolfe M. Intramembrane proteolysis by presenilin and presenilin-like proteases. J Cell Sci. 2003; 116:2839–2844. [PubMed: 12808018]

Yang T, Arslanova D, Gu Y, Augelli-Szafran C, Xia W. Quantification of gamma-secretase modulation differentiates inhibitor compound selectivity between two substrates Notch and amyloid precursor protein. Mol Brain. 2008; 1:15. [PubMed: 18983676]

Yu G, Nishimura M, Arawaka S, et al. Nicastrin modulates presenilin-mediated notch/glp-1 signal transduction and betaAPP processing. Nature. 2000; 407:48–54. [PubMed: 10993067]

Zetterberg H, Campbell WA, Yang HW, Xia W. The cytosolic loop of the gamma -secretase component presenilin enhancer 2 (Pen-2) protects zebrafish embryos from apoptosis. J Biol Chem. 2006; 281:11933–11939. [PubMed: 16507571]

Zhong TP, Childs S, Leu JP, Fishman MC. Gridlock signalling pathway fashions the first embryonic artery. Nature. 2001; 414:216–220. [PubMed: 11700560]

Zon LI, Peterson RT. In vivo drug discovery in the zebrafish. Nat Rev Drug Discov. 2005; 4:35–44.
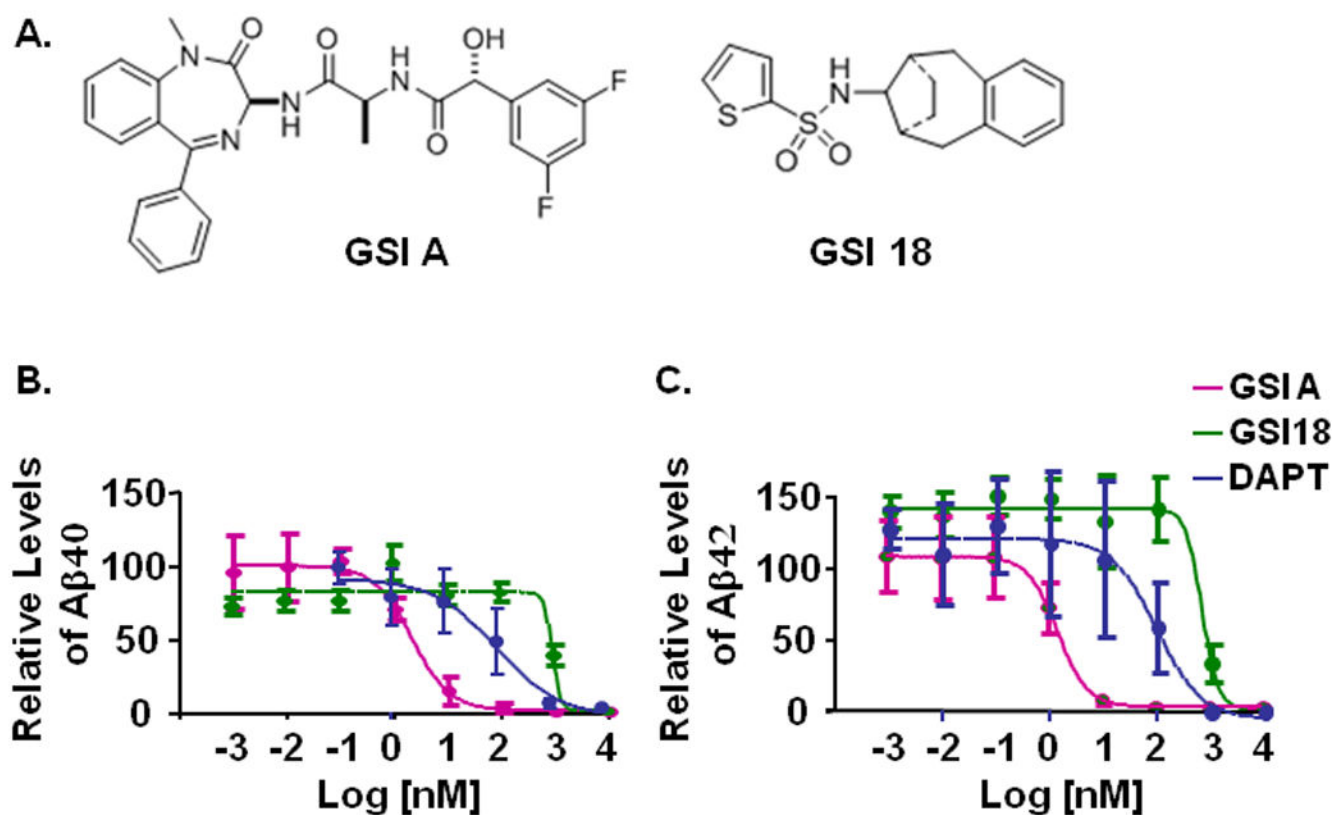[PubMed: 15688071]

Fig. 1. The structures of GSI A and GSI 18 and an inhibition of γ-secretase cleavage of APP
A. The structures of GSI A and GSI 18. **B**. An APP overexpressing CHO cell line 7W was treated with individual compounds and the levels of secreted Aβ in the media were measured by ELISA. Levels of Aβ in the media of 7W cells that were treated with 0.1% DMSO were normalized to 100% and used to calculate the relative levels of Aβ40 (left panel) and Aβ42 (right panel) from cells treated with GSI A, GSI 18, or DAPT. Standard errors of means are illustrated by bars.
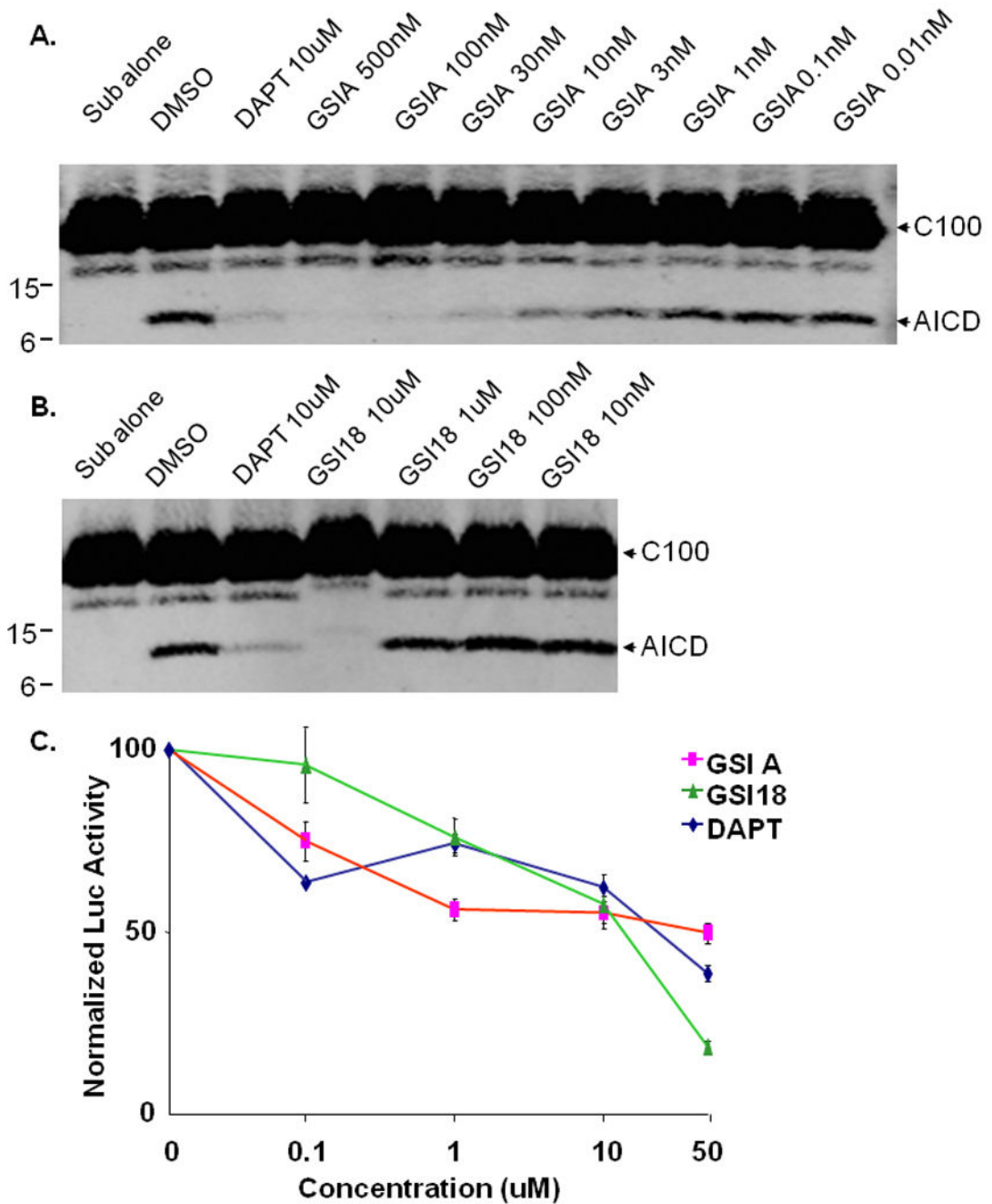
Fig. 2. GSI A and GSI 18 inhibit APP AICD generation and Notch NICD induced luciferase reporter gene expression

The *E. coli* generated APP-based, 100-residue γ-secretase substrate C100-Flag was mixed with the membrane vesicles solubilized in CHAPSO after DMSO or compounds were added. The mixture was incubated at 37°C for 4 hours. **A**. An inhibition of AICD generation by GSI A was detected by Western blot (WB) with Flag antibody. **B**. Generation of AICD was inhibited in the presence of 10 μM of GSI 18. DAPT at 10 μM also inhibited AICD generation, while substrate alone ("Sub alone", in the absence of γ-secretase) was not

converted to AICD. **C**. A *Hes-1* reporter construct (Hes-Luc) containing Notch NICD targeting sequence was transfected into HEK293 cells, followed by treatment with different concentrations of GSIs. The level of luciferase activity in cells treated with DMSO was normalized to 100%, and relative luciferase activities representing NICD levels were quantified in cells treated with different concentrations of GSI A, GSI 18 or DAPT. Error bars represent the standard errors of means.
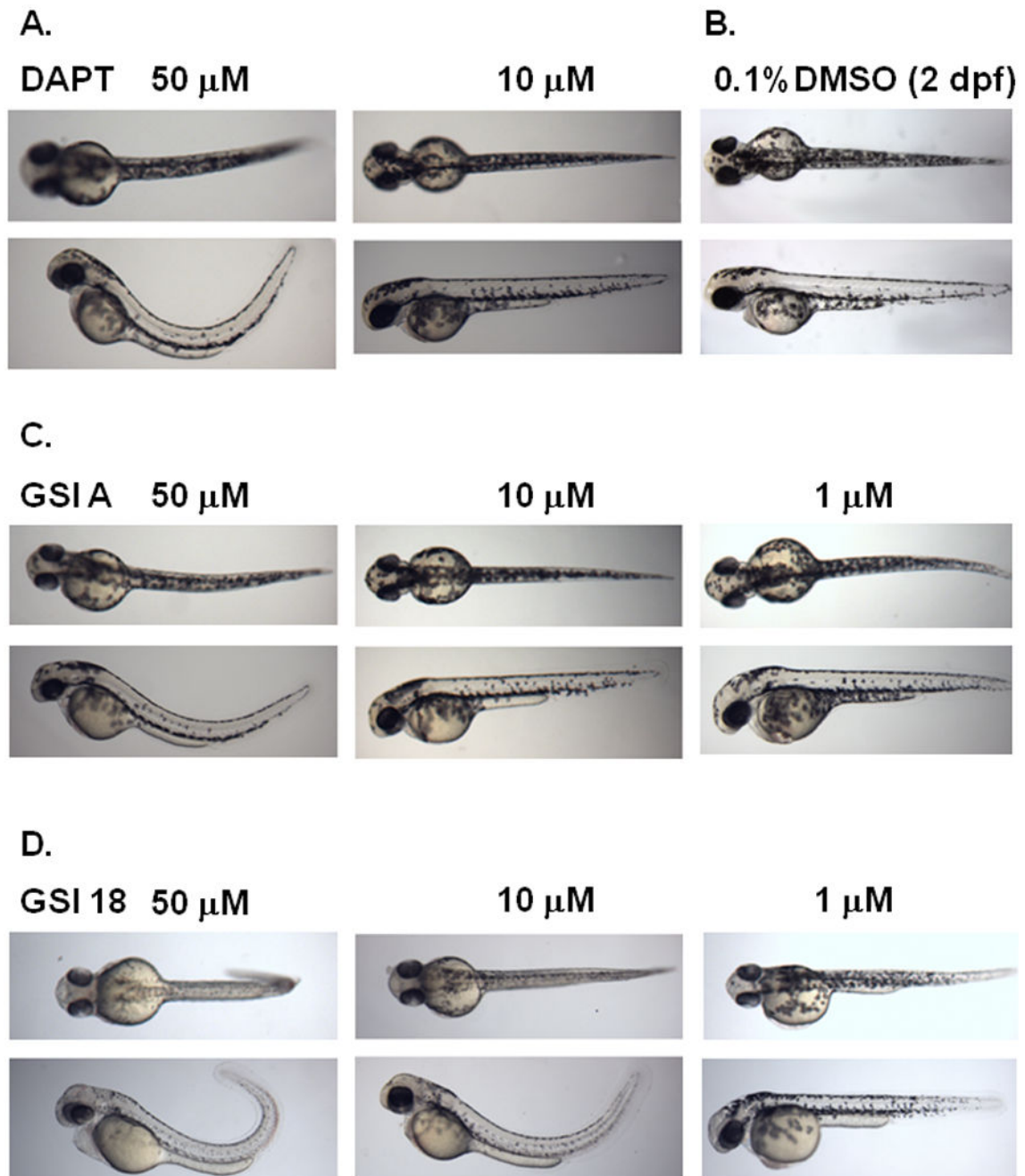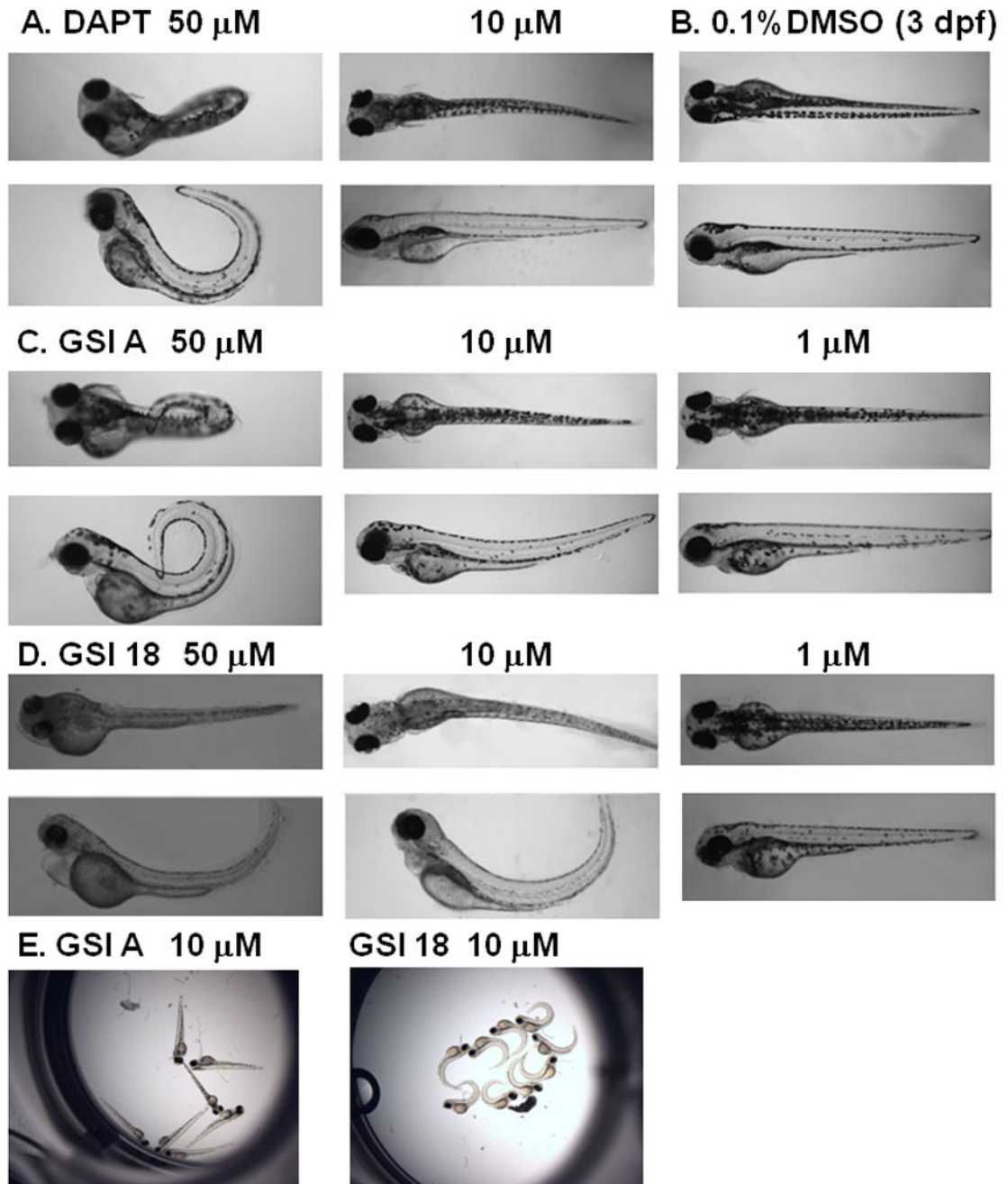
Fig. 3. Phenotype alteration at 2 dpf in embryos treated with increasing concentrations of GSI A or GSI 18
Embryos were treated at 24 hpf, and dorsal (top panel) and lateral (bottom panel) views of embryos were acquired at 2 dpf. DAPT is a previously reported GSI that caused curved tail at 50 μM but not 10 μM (**A**), compared to control embryos treated with 0.1% DMSO that show a wild-type phenotype (**B**). Three concentrations of GSI A (**C**) and GSI 18 (**D**) were used to treat zebrafish embryos at 24 hpf.

Fig. 4. Phenotype alteration at 3 dpf in embryos treated with increasing concentrations of GSI A or GSI 18

A. Embryos treated with 50 μM DAPT showed a strong phenotype, and much less effect was observed at lower concentration of 10 μM. **B**. DMSO treated embryos did not reveal any phenotype at 3 dpf. **C**. GSI A was used at 50 μM, 10 μM, and 1 μM. In contrast to embryos treated with 50 μM GSI A, 10 μM and 1μM of GSI A did not cause phenotype alteration. **D**. All embryos showed clear curved tails in 50 μM GSI 18. Embryos treated with 10 μM of GSI 18 still showed similar morphologic changes, and much less effect was

observed at lower concentration of 1μM. **E,** All embryos treated with 10 μM GSI A showed normal phenotype similar to DMSO treated embryos. On the contrary, all embryos treated with 10 μM GSI 18 showed much stronger phenotypic alteration.
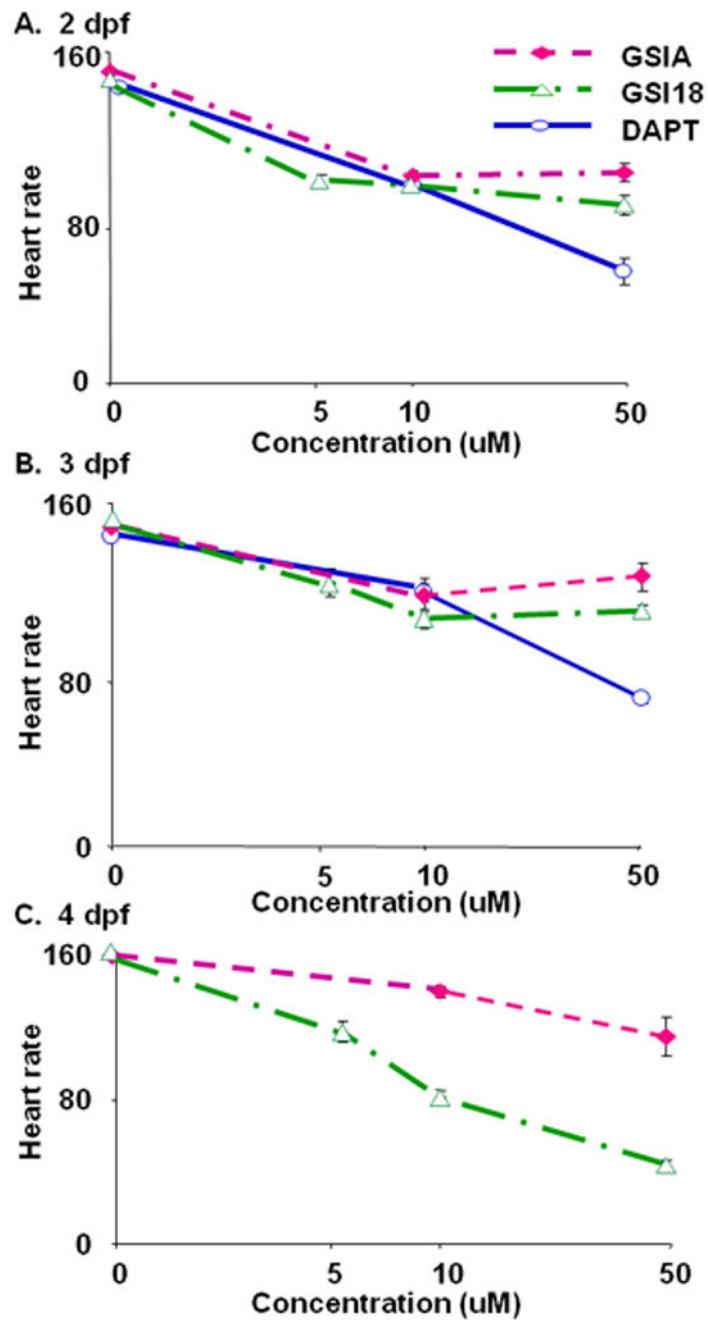
Fig. 5. Heart rate analysis of zebrafish embryos

Embryos treated with GSIs were kept for 4 days post fertilization (dpf). The embryos were placed on their side for videotaping, and the heart rate, in beats per minute, was determined by extrapolating the number of heart beats per 15 sec on the video. The average heart rates for GSI A or GSI 18 treated embryos were similar during 2–3 dpf (**A, B**), but the rate for GSI 18 treated embryos was dramatically reduced compared to GSI A treated fish and controls at 4 dpf (**C**). DAPT-treated embryos failed to show clear heart beats at 4 dpf (**C**).
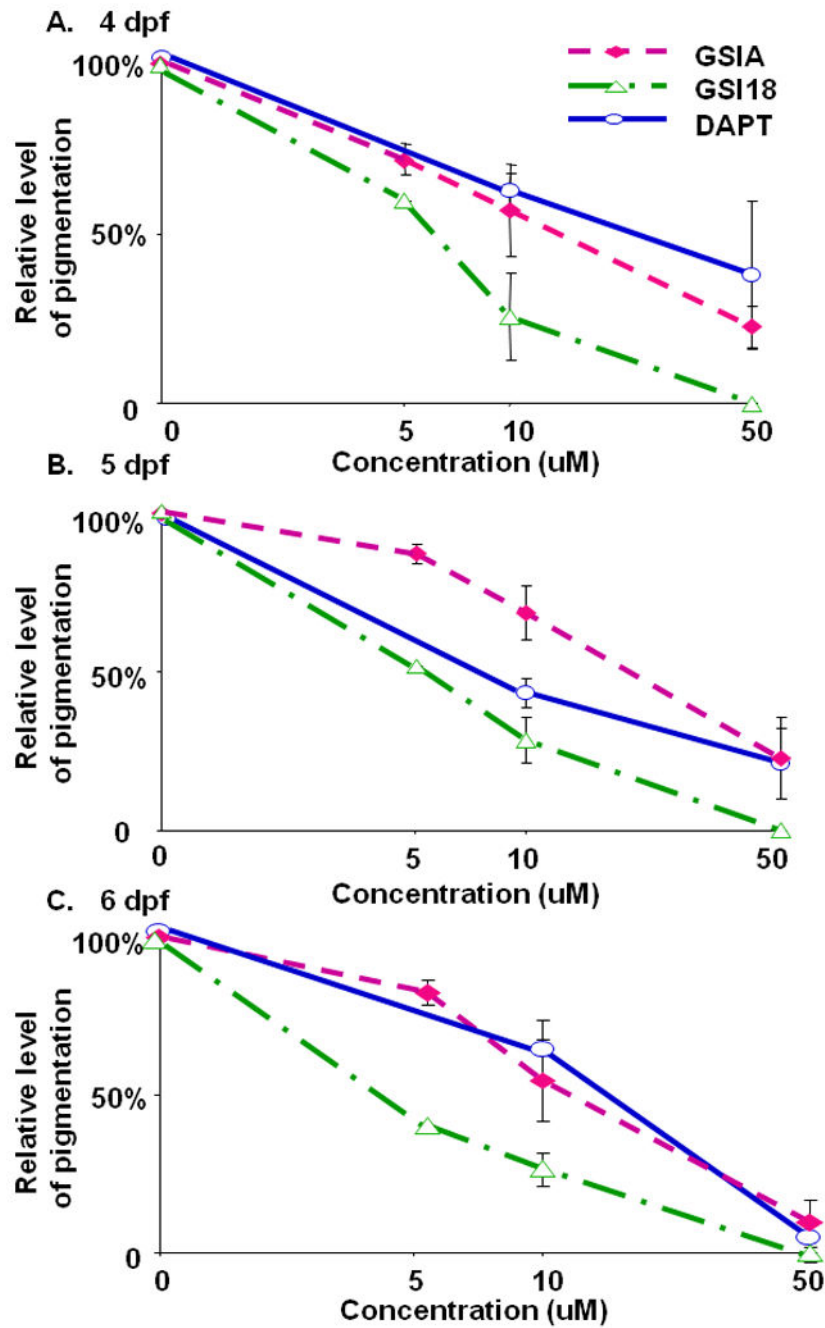
Fig. 6. Relative levels of pigmentation in embryos treated with GSIs

The region of interest that illustrates pigmentation was manually drawn and segmented. The intensity of pigmentation (the total area and average pixel values of pigmentation) was quantified, and the value of the DMSO treated embryos was used as the benchmark for comparison. The level of pigmentation of embryos treated with DMSO was defined as 100%. Embryos treated with GSI 18 at 50 μM were transparent, and the level of pigmentation was defined as 0. The relative levels of pigmentation of other GSI-treated embryos were scaled between 0 and 100%. Error bars represent the standard error of means.
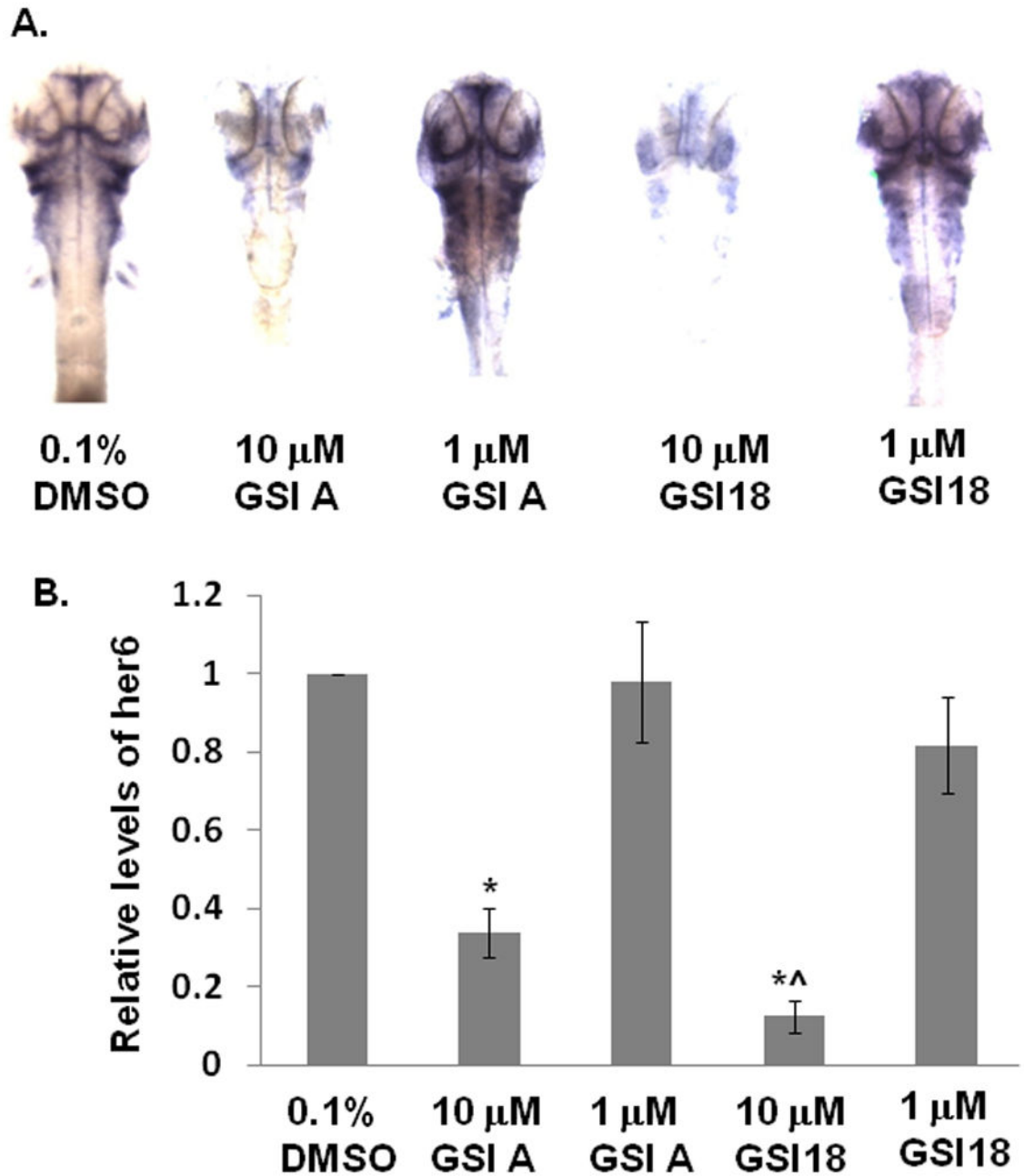
Fig. 7. Effect of GSIs on Notch signaling *in vivo*
A. GSI A or GSI 18 at 10 and 1 μM were applied to dechorionated zebrafish embryos at 24 hpf, then the embryos were fixed at 48 hpf in 4% formaldehyde. *In situ* hybridization was performed to stain *her6* expression. At least 10 to 20 embryos were examined for each experiment. Images were taken at the 64x magnification for stained embryos. In control embryos, *her6* expression was abundant in the dorsal diencephalon, retinas, ventral midbrain and ventral hindbrain. The intensity of *her6* staining was reduced when 10 μM of GSI A or GSI 18 were used to treat embryos. Embryos treated with 1 μM of GSIs did not reveal much

difference from DMSO treated embryos. **B**. Different regions with *her6* expression as described above were segmented and the intensity of individual regions was quantified. The expression levels of *her6* in DMSO treated zebrafish were normalized to 1, and the relative levels of *her6* expression in GSI-treated embryos were calculated. Embryos treated with 10 μM GSI A or GSI 18 showed a significant reduction in relative levels of her6 expression compared to DMSO-treated embryos (indicated by *). A significant lower level of her6 expression was found in 10 μM GSI 18-treated embryos, compared to 10 μM GSI A-treated embryos (indicated by ^).